Effect of spatial variability on undrained behaviour of tunnel with improved surroundings

Yutao PAN
Research Fellow, Dept. of Civil and Environmental Engineering, National University of Singapore, Singapore

Fook Hou LEE
Professor, Dept. of Civil and Environmental Engineering, National University of Singapore, Singapore

ABSTRACT: Cement treated ground is extensively used to limit ground disturbance during tunneling in soft soils in Singapore. The cement treated columns are installed in an overlapping fashion to form a circular surrounding which resists the deformation during excavation. In practical design, the cement treated ground is usually assumed to be homogenous and elastic-perfectly plastic although it is highly spatially variable and exhibits significant strain softening and hardening behaviours. In this study, random finite element method (RFEM) is used to account for the effect of spatial variability of unconfined compressive strength of cement treated soil. The complex constitutive behaviour is simulated using the Cohesive Cam Clay (C3) model which is developed to describe the complex hardening and softening constitutive behaviour. The critical state is defined as the moment when volume loss suddenly increases and the critical stress release ratio is marked. A parametric study was conducted to find the relationship between quality control parameters and equivalent strengths. A rational guideline on design strength is provided based on the probabilistic distribution of equivalent strength.

1. INTRODUCTION

To minimise the ground disturbance due to tunnelling in clayey grounds, cement-treatment is commonly used to create a zone of hardened soil around the tunnel periphery to prevent soil collapse (e.g. Pellegrino and Adams, 1996, O' Rourke and McGinn, 2006; Ochmanski et al. 2015). Similar improved soil surrounds have also been used when tunnelling through marine clay in Singapore. The presence of this improved soil surround is likely to affect the failure modes and stability characteristics of the tunnel significantly (Tyagi et al. 2017).

In geotechnical design, cement-treated soil is often modelled as a uniform Tresca-material (e.g. Yang et al. 2011). In reality, the behaviour of cement-treated clay is often marked by significant degree of strain softening (e.g. Xiao et al. 2016;). Cement-treated soil mass also often exhibits significant spatial variability in strength (e.g. Larsson et al. 2005ab, Liu et al. 2015, 2017, 2018; Chen et al. 2016; Pan et al. 2017, 2018a, b c & d).

Previous studies on the effects of spatial variability of cement-treated clay includes global strength of an axially-loaded cement-treated column (Namikawa and Koseki, 2013) as well as global strength and stiffness of cement-treated clay slab for excavation support (Liu et al., 2015; Pan et al. 2018b). Both studies used Tresca model in their analyses. Tyagi et al. (2018) also studied the effect of spatial variability on the performance of improved soil zone around tunnel using a Mohr-Coulomb model. None of these studies took into account the strain softening behaviour of cement-treated clay. Pan et al. (2018a) used a randomized version of Xiao et al.'s (2016) Cohesive Cam Clay (C3) model to study the compressional behaviour of spatially variable cement-treated columns. However, the stress state in the column is predominantly compression and is unlikely to be representative of that in an

improved soil zone around a tunnel, which is subjected to both compression and flexure (Tyagi et al. 2017). The effect of spatial variability and strain softening on the stability and deformation of improved soil zones around tunnels is still not well understood.

This paper examines the combined effect of spatial variability and strain-softening on the short-term undrained stability and deformation of a tunnel cross-section with an improved soil ring around it, hereafter termed "improved soil surround", as illustrated in Fig. 1. The modelling methodology is first described. The results showed that, compared to a cement-treated soil slab for excavation, a smaller strength reduction factor is required for tunnel improved soil surround. This leads to a method for estimating the design strength of the cement-treated soil taking into account the spatial variability and strain softening.

2. PROBLEM DESCRIPTION AND MODEL SETUP

2.1. Problem Description

The random finite element analyses were conducted using a modified version of GEOFEA (www.geosoft.com.sg), using a randomised version of Xiao et al.'s (2016) C3 model (Pan et al. 2018a-c). As Fig. 2 shows, a tunnel cross-section was analysed assuming plane strain conditions. This is conservative from the perspective of the tunnel wall since it ignores the supporting effect of the soil in front of the face and is still commonly employed in practice (e.g. Sharma et al. 2001; Tyagi et al. 2017, 2018). It also simulates a scenario of an excavated tunnel some distance behind the tunnel face. By incorporating spatial variation in the improved soil properties, a direct comparison between randomly variable and uniform soil conditions can be made. This, in turn, permits an equivalent set of properties to be prescribed for an equivalent uniform medium in two-dimensional plane strain analyses. Following Tyagi et al. (2017), the parametric study covers three geometric parameters, namely the embedment depth C, excavated tunnel diameter D and thickness of improved soil surround t, Fig. 2, as well as the properties of the improved soil surround and soft soil.

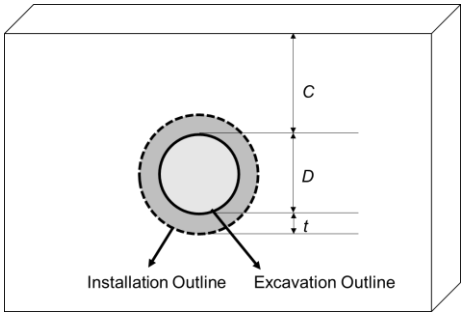

Fig. 1 Geometrical configurations

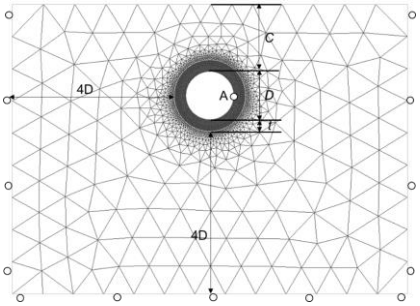

Fig. 2 Typical Mesh Layout, mesh for random finite element study (mesh size of improved surround=0.3m; Point A marks the spring line)

2.2. Finite Element Model

The finite element mesh comprises 3800 linear strain triangular elements. A finer mesh is used for cement treated soil surround due to the high stress concentration. Preliminary studies show that the mesh size of 0.3 m of the improved surround would give a convergent result in both deterministic and random scenario. The bottom boundary was fixed against all movements while the side boundaries were fixed against horizontal displacement. Tunnel excavation was modelled by removing soil elements from inside the tunnel opening. In this study, 100 excavation increments were used, so that each increment represents 1% decrease in tunnel support pressure. The progress of the excavation is represented by a stress release ratio, which is defined as the ratio of decrease in tunnel support pressure at the current increment to the full support pressure. The stress release ratio is thus zero before excavation and 100% upon completion of tunnel excavation.

Since tunnel deformation is non-uniform, a single-value parameter, the volume loss ratio, is used to quantify the overall deformation of the tunnel. As Fig. 3 shows, the volume loss ratio is the ratio of the decrease in tunnel cross-section area to the original cross-sectional area, and is a measure of tunnel convergence. In the analysis, it was evaluated by the ratio of the average inward radial displacement of the nodes around the tunnel to the initial radius.

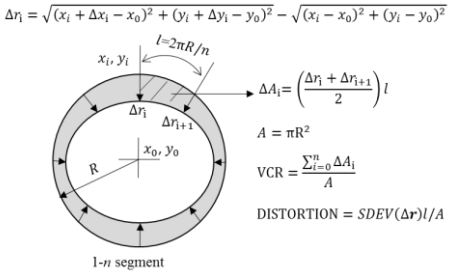

Fig. 3 Illustration of Volume Change Ratio (VCR) and Distortion.

2.3. Constitutive model

The soft clay was modelled using the modified Cam Clay model, parameters summerised in Table 1. The cement-treated clay was modelled using C3 model, Fig. 4 (Xiao et al. 2016). Details of the C3 model has been reported by Xiao et al. (2016) and Pan et al. (2016, 2018a) and will not be repeated herein. Following Pan et al. (2018a), the parameters of the C3 model were correlated to unconfined compressive strength (qu), Table 1.

Table 1 Model parameters for this study

Marine Clay	Modified Cam Clay Model
κ=0.06 λ=0.244 M=0.9 e_{cs}=2.221 μ'=0.33 γ_{bulk} =16 kN/m^3 OCR=3 and K_0=1.0 (for the hard crest) OCR=1 and K_0=0.7 (for the underlying clay)	
Cement-treated Clay	C3 Model
κ=0.01; λ_i=0.25; M=2.4; V_0=3.35; μ'=0.2; α=2.2; β=0.28; γ_{bulk} =16 kN/m^3; $C_i = 0.36q_u$; $p_{py} = 0.62q_u$; $\sigma_t = 0.13q_u$; q_u varies in each case	

2.4. Verification

To verify the numerical model with C3 model, the numerical results were compared with Tyagi et al.'s (2017) centrifuge test results on tunnels with uniform improved soil surrounds, using the prototype equivalent dimensions of Tyagi et al.'s (2017) experiments.

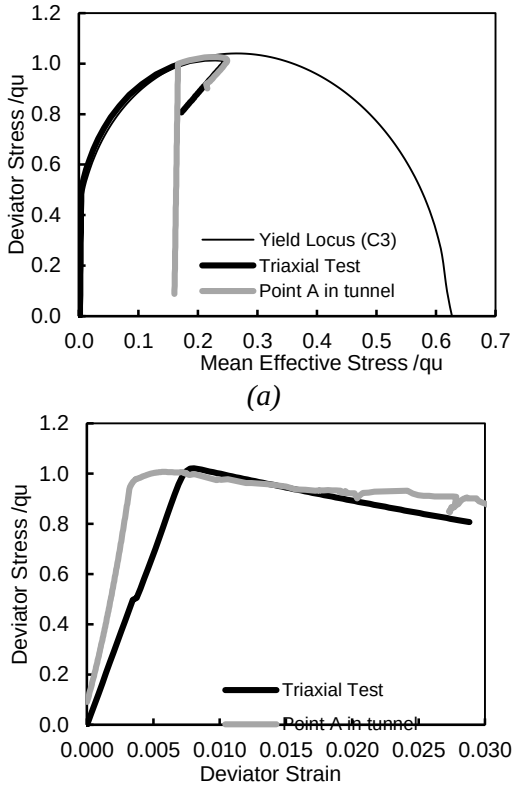

Fig. 4 Behaviour of C3 model in triaxial test and tunnel spring line: (a) stress paths; (b) stress strain curves (Point A is marked in Fig. 2)

Table 2. Centrifuge test details for single large diameter tunnels in improved soil surround (Source: Tyagi et al., 2017)

Case	Diameter (D) /m	C/D	Thickness ratio (t/D)	Strength kPa
V1	15	1.00	0.2	600
V2	11	1.60	0.27	606
V3	12	1.42	0.33	600
V4	11	1.64	0.27	732
V5	12	1.42	0.33	1440
V6	15	1.00	0.2	452
V7	11	1.64	0.45	440

The critical state defined in Tyagi et al. (2017) corresponds to a state of incipient collapse, which is marked by an abrupt stress change at the interface between improved soil surround and soft soil. In finite element analyses, failure may be more directly tracked using global indicators of tunnel response. Fig. 5(a) shows the computed volume loss response with stress release ratio for Tyagi et al.'s (2017) tests summarized in Table 2. With the exception of Case V5, all volume loss curves show an initial linear portion followed by a flattening that indicates increasing rapid volume

loss. In Case V5, the volume loss ratio showed no transition point and out-of-balance load remains below 1% throughout the tunnel excavation as the strength of the improved soil surrounding is very high. Failure was also not observed in the centrifuge test. Fig. 5(b) compares the critical stress release ratio corresponding to the first departure from linearity with Tyagi et al.'s (2017) critical stress release ratios. As can be seen, the critical stress release ratios obtained by the two approaches are in reasonably good agreement. Hence, the transition point for the volume loss will be used as an indicator of failure hereafter.

2.5. Relationship between unconfined compressive strength and critical stress release ratio

As Fig. 6 shows, with the same strength of improved surrounding, the critical stress release ratio increases proportionally with unconfined compressive strength of the homogeneous improved surround. This is not surprising because when the unconfined compressive strength of the improved surrounding is very low, the size of C3 yield locus is so small that any disturbance in ground would lead to failure.

Hence simple empirical linear relationship can be evaluated,

$$q_{\mathrm{ud}} = 588 R_{\mathrm{cd}} \qquad (1)$$

where

q_{ud} - the unconfined compressive strength of the improved surrounding;

R_{cd} - the critical stress release ratio as defined above;

Eq. 5 links the unconfined compressive strength with the critical stress release ratio. As will be shown later, when a critical stress release ratio is known, its equivalent strength can be readily evaluated. It goes without saying that the relationship between the strength and the critical stress release ratio varies with geometric configurations (diameter, thickness, embedment depth, etc.) of the tunnel surround. In this paper, only one simple case is examined. On the other hand, with a strength higher than 600 kPa, the critical stress release ratio should be 1 and the linearity is not conformed. Nevertheless, the current study is interested in the degradation ratio of random case from deterministic case.

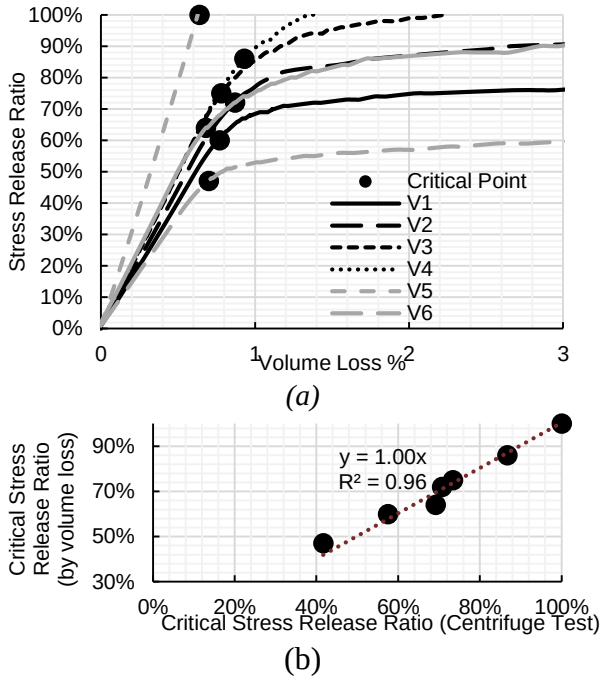

Fig. 5 Verification with centrifuge test data, (a) stress release ratio vs volume loss ratio curve (the black dots indicate the onset of sharp increase of volume loss); (b) stress release ratio marking the onset of sharp increase of volume loss [black dots in subplot (a)];

3. EFFECT OF SPATIAL VARIABILITY ON STABILITY AND DEFORMATION OF TUNNEL WITH IMPROVED SURROUNDING

Spatial variability of the improved soil surround was simulated using a two-dimensional random field with marginal PDF of lognormal distribution, which was generated using the Modified Linear Estimation Method (MLEM) (Liu et al. 2014). The plane strain nature of the problem implies that the SOF in the out-of-plane direction is infinitely long, which is counter-intuitive. The horizontal and vertical SOF are assumed to be equal to the thickness of improved soil surround.

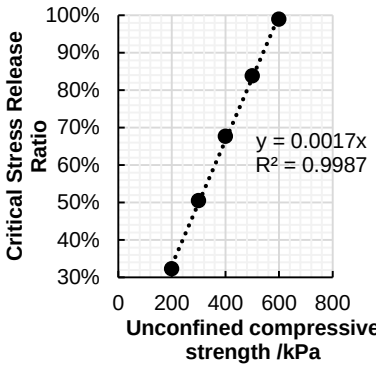

Fig. 6 Parametric study in deterministic analysis

The undrained shear strength of the surrounding untreated soil is assumed to increase with depth with a deterministic trend. As the improved soil surround has much higher strength and modulus (Lee et al. 2005; Xiao et al. 2014) than the surrounding soft soil, the variability of the former will have a much greater effect on the stability of the tunnel. It is also in line with the main focus of this paper.

3.1. Typical Results – Reference Case

Fig. 7 (a) shows the contours of unconfined compressive strength of one realization under three stages of loading. In underground construction stabilization works, the mean strength of cement-treated soft clay typically ranges from 1MPa to 2MPa. However, a much lower mean strength of 600kPa is used herein so as to enable tunnel collapse. As Fig. 7(b) shows, the volume loss firstly increases linearly with stress release ratio at the initial stage, through Point A to Point B. Softening has already initiated in the weak zone even at the initial stages. However, the zones remain isolated and none of them covered the entire thickness of the improved soil surround, Fig. 7(c). At Point B, the volume loss curve shows acceleration in volume loss. The largest softened zone has also just extended through the thickness of the improved soil surround. This indicates that softening has now covered the entire thickness at one location of the circumference of the improved soil surround. Further enlargement of the softened zones continues to occur through Point C and beyond, as other locations along circumference are gradually mobilized. Hence Point B can be regarded to be point of incipient failure (Tyagi et al. 2017). The stress release ratio at Point B is defined herein as the critical stress release ratio.

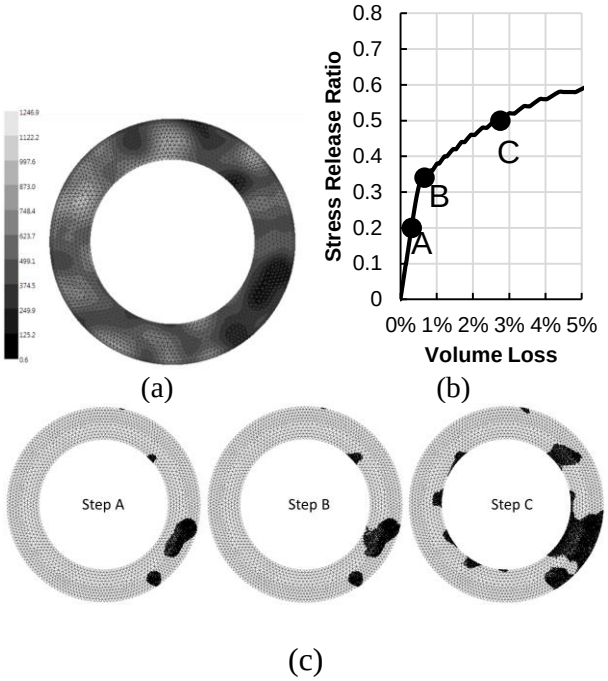

Fig. 7 One typical realization with mean value=600kPa, COV=0.4, SOFx=SOFy=3m, (a) random field of unconfined compressive strength; (b) stress release ratio vs volume loss curve; (c) distribution of softened points at different points.

As Fig. 8(a) shows, the volume loss curves of all the other realizations show a similar trend. All of the random realisations have lower critical stress release ratios than the deterministic analysis. This is because softening initiates from

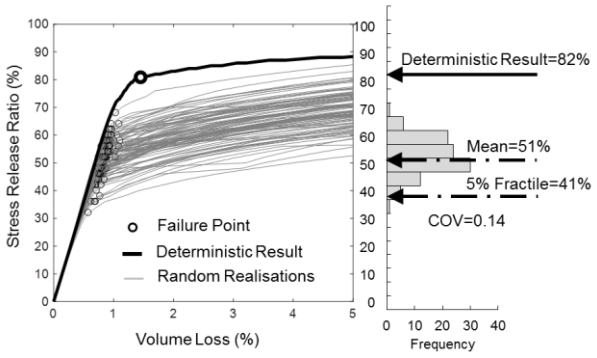

Fig. 8 typical random results for a tunnel with D=12m, t/D=0.25, C/D=1.4, input COV=0.4 and SOF/t=1.0 m)

the weak zones where the strength is invariably lower than the mean strength. Similar findings can be found in other random finite element studies (Namikawa and Koseki, 2012; Ching and Phoon, 2013; Liu et al. 2015; Pan et al. 2018abc). Based on a histogram of the critical stress release ratio, a mean and a 5% fractile of the critical stress ratios can be evaluated from the random analyses, Fig. 8(b). Preliminary study showed that 100 realisations were sufficient to make a convergent mean and COV of the random results.

3.2. Effect of Scale of Fluctuation.

The effect of scale of fluctuation (SOF) can be evaluated by evaluating Case R1 through R6, the mean critical stress release ratio initially decreases, and then increases slightly with the SOF, with the minimum value occurring at an SOF of approximately one time the thickness. This is not surprising; the strength of the cement-treated soil is significantly correlated within a distance of approximately 1 SOF. Thus, this is also roughly the typical size of a weak zone. When the size of the weak zone is approximately equal to the thickness of the improved soil surround, softening is also likely to occur over the entire thickness of the improved soil surround. As discussed above, this is the point at which the volume loss curve starts to depart from linearity. The 5% fractile of the critical stress ratio decreases monotonically with SOF, stabilizing when the SOF is approximately equal to the thickness of the improved soil surround.

On the other hand, the COV of the critical stress release ratio, hereafter termed "output COV", increases monotonically with SOF. As the SOF increases, the local averaging effect diminishes and the critical stress release ratio tends to approach the COV of the cement-treated soil, hereafter termed input COV. Similar findings have been reported by Namikawa and Koseki, (2013), Pan et al. (2018a & b) and Tyagi et al. (2018). Liu et al. (2018) noted that there are two ranges of SOF in cement-treated soil mass. The first is a short-range SOF which is related to the quality of mixing while the second is a long-range SOF which is related to the variation in in-situ moisture content. The latter varies considerably with the in-situ soil type, but may be of the order of tens of metres (e.g. Phoon and Kulhawy, 1999). The SOF of the in-situ soil properties is not considered herein. The short-range SOF is typically much smaller than the diameter of a deep-mixed column and is therefore much smaller than the thickness of the improved soil surround. For the parametric study, the SOF is kept equal to the thickness of the improved soil surround, to ensure that the results are conservative with respect to SOF.

3.3. Effect of Mean Value and Input COV.

In Cases R1-R6, R9-R10, the random cases use a mean unconfined compressive strength of 600 kPa to ensure the occurrence of failure in the current configuration. By comparing Case R1, R7 & R8 in Table 3, one finds that the normalised mean critical stress release ratio (NMSRR) increases while the output COV decreases. This is mainly because when the mean strength is high, some of the realisations do not fail. The unfailing realisations all gives 100% stress release ratio despite the differences among them. As such, the output COV of critical stress release ratio reduces and the normalised mean value of critical stress release ratio increases as the mean unconfined compressive strength increases.

Expectedly, as the input COV increases, the mean value of critical stress release ratio reduces significantly, while the output COV only increases slightly, Cases R9-10. This shows the effect of quality control on the global behaviour of spatially-variable improved surrounding.

4. DESIGN IMPLICATIONS

In engineering practice, it is usually very difficult for engineers to use random finite element method which is far more time-consuming and complex than traditional deterministic analysis. One practical alternative is to assume the improved surrounding is homogeneous with a discounted equivalent strength. This section aims at proposing a rational guideline for design of tunnel with improved surrounding based on the findings. The

approximate relationship between equivalent strength and critical stress release ratio is firstly established. Then a design approach is proposed based on the findings. An illustration example is given to facilitate usage of the design charts.

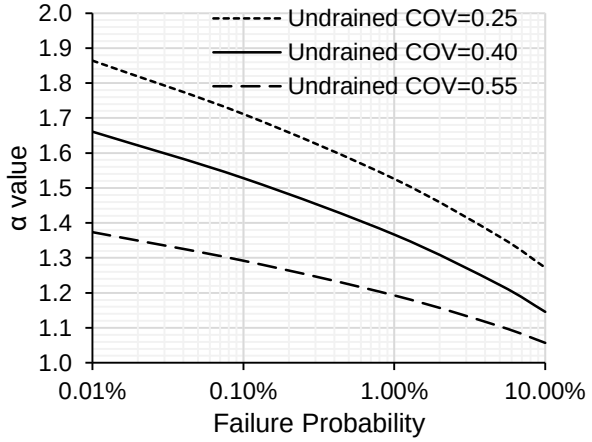

Fig. 9 Design graph for reduction factor

4.1. Equivalent Strength

The above discussion shows that the existence of random spatial variability reduces the critical stress release ratio from the homogeneous counterpart. In effect, it amounts to a discount on the strength. For each random realisation, there is an equivalent representative strength with which the deterministic analysis can give the same critical stress release ratio. The same procedure for evaluating equivalent strength is given in Pan et al. (2018c). The equivalent strength is normalised by the mean unconfined compressive strength,

$$\eta = \frac{q_{\mathrm{u\_eq}}}{q_{\mathrm{u\_ave}}} = \frac{R_{\mathrm{cr}}}{R_{\mathrm{cd}}} \tag{2}$$

where η is the normalised equivalent strength, Rcr the critical stress release ratio in random case, Rcd the critical stress release ratio in deterministic (homogeneous) case.

4.2. Design Approach

The design value should be a representative value from a spectrum of equivalent strength which is rationally conservative. In design, a fractile is usually used as the representative value of a given distribution (Liu et al. 2015, Toraldo et al. 2017; Pan et al. 2017, 2018bcd). For example, 5% fractile of a given sample space is smaller than 95% of all samples. In this study, the characteristic value can be evaluated as:

$$q_k = A q_{\mathrm{u\_ave}}(1-\beta B) \tag{3}$$

where

q_{k} -characteristic value of unconfined compressive strength of improved surrounding;

A- mean value of normalised equivalent strength; for C3 and Tresca model, it is equal to NMSRR, as listed in Table 3; for Mohr-Coulomb model, the mean normalised equivalent strength are listed in brackets.

$q_{\mathrm{u\_ave}}$-mean value of unconfined compressive strength from field data;

B-output COV of critical stress release ratio; for C3 and Tresca model, it is equal to NMSRR, as listed in Table 3; for Mohr-Coulomb model, the mean normalised equivalent strength are listed in brackets.

β- reliability index (BSI, 2002), it depends on the probability of failure (p),

$$\beta = \Phi^{-1}(p) \tag{4}$$

Alternatively, one can evaluate the characteristic strength directly from the mean and standard deviation of coring strength (Liu et al. 2015).

$$q_k = \overline{q_u} - \alpha\sigma \tag{5}$$

where

σ - the standard deviation of unconfined compressive strength of coring samples.

α – the strength reduction factor. Substituting Eq. 10 into Eq. 8 gives:

$$\alpha = \frac{1 - A(1-\beta B)}{\sigma / q_{\mathrm{u\_ave}}} \tag{6}$$

The strength reduction factor can be evaluated from Fig. 9.

Table 3 Parametric studies in two-dimensional random analysis

No.	SOF/*t*	Mean q_u	COV of q_u*	Normalized critical stress release ratio (Undrained)		
				NMSRR**	Output COV	N5SRR
R1	1	600	0.4	0.63	0.13	0.50
R2	1/6	600	0.4	0.70	0.04	0.65
R3	1/3	600	0.4	0.65	0.06	0.58

R4	2/3	600	0.4	0.63	0.11	0.52
R5	4/3	600	0.4	0.64	0.15	0.50
R6	8/3	600	0.4	0.68	0.18	0.50
R7	1	1200	0.4	0.88	0.14	0.68
R8	1	1700	0.4	0.99	0.03	0.93
R9	1	600	0.25	0.76	0.09	0.65
R10	1	600	0.55	0.51	0.15	0.39

* Input COV means the COV of unconfined compressive strength; Output COV means the COV of the critical stress release ratio.
** NMSRR is the normalized mean stress release ratio, it is defined as the ratio of mean critical stress release ratio normalised by the corresponding result from an analysis that assumed a uniform improved soil surround with the mean strength; N5SRR is the normalized 5% fractile stress release ratio, it is defined as the ratio of 5% fractile of critical stress release ratio normalised by the corresponding result from an analysis that assumed a uniform improved soil surround with the mean strength.

5. CONCLUSIONS

Spatial variability has a significant adverse effect on the short-term undrained stability of tunnel with improved surrounding. When 5% fractile is used as a rationally conservative value, a discount of as low as 39% may be applied on the mean unconfined compressive strength, depending on the COV of point strength. A rational design approach is proposed for easy reference of equivalent strength assuming the improved surrounding is deterministic and homogeneous.

6. REFERENCES

BSI 2002. EN 1990:2002 – Eurocode, Basic of Structural Design, European Committee for Standardization. Brussels

Chen, J., Liu Y., & Lee, F.H. (2016). A statistical model for the unconfined compressive strength of deep mixed columns. Geotechnique. 66(5): 351-365.

Ching, J., & Phoon, K. K. (2013). Mobilized shear strength of spatially variable soils under simple stress states. Structural Safety, 41, 20-28.

Larsson, S., Dahlstrom, M., & Nilsson, B. (2005a). Uniformity of lime-cement columns for deep mixing: a field study. Ground Improvement, 9(1), 1-16.

Lee, F. H., Lee, Y., Chew, S. H., & Yong, K. Y. (2005). Strength and modulus of marine clay-cement mixes. Journal of geotechnical and geoenvironmental engineering, 131(2), 178-186.

Liu, Y., Lee, F.H., Quek, S.T. and Beer, M., 2014. Modified linear estimation method for generating multi-dimensional multi-variate Gaussian field in modelling material properties. Probabilistic Engineering Mechanics, 38, pp.42-53.

Liu, Y., Lee, F.H., Quek, S.T., Chen, E.J. and Yi, J.T., 2015. Effect of spatial variation of strength and modulus on the lateral compression response of cement-admixed clay slab. Géotechnique, 65(10), pp.851-865.

Namikawa, T., & Koseki, J. (2013). Effects of Spatial Correlation on the Compression Behaviour of a Cement-Treated Column. Journal of Geotechnical and Geoenvironmental Engineering, 139(8), 1346-1359.

Pan Y, Xiao Huawen, Lee Fook Hou, Phoon Kok Kwang (2016). Modified Isotropic Compression Relationship for Cement-Admixed Marine Clay at Low Confining Stress. Journal of Geotechnical Testing Journal, 39(4), 695-702.

Pan, Y., Liu, Y., Hu, J., Sun, M., & Wang, W. (2017). Probabilistic investigations on the watertightness of jet-grouted ground considering geometric imperfections in diameter and position. Canadian Geotechnical Journal, (ja).

Pan, Y., Liu, Y., Xiao, H., Lee, F. H., & Phoon, K. K. (2018a). Effect of spatial variability on short-and long-term behaviour of axially-loaded cement-admixed marine clay column. Computers and Geotechnics.

Pan, Y., Liu, Y., & Chen, E. J. (2018b). Analysis of Cement-treated Soil Slab for Deep Excavation Support – A Rational Approach. Géotechnique, (accepted).

Pan, Y., Shi, G., Liu, Y., & Lee, F. H. (2018c). Effect of spatial variability on performance of cement-treated soil slab during deep excavation. Construction and Building Materials, 188, 505-519.

Pan, Y., Liu, Y., & Chen, E. J. (2018d). Probabilistic investigation on defective jet-grouted cut-off wall with random geometric imperfections. Géotechnique, 1-49..

Phoon, K. K., & Kulhawy, F. H. (1999). Characterization of geotechnical variability. Canadian Geotechnical Journal, 36(4), 612-624.

Tyagi, A., Zulkefli, M. F. B., Pan, Y., Goh, S. H., & Lee, F. H. (2017). Failure modes of tunnels with improved soil surrounds. Journal of Geotechnical and Geoenvironmental Engineering, 143(11), 04017088.

Tyagi, A., Liu, Y.., Pan, Y., Ridhwan, K. B. M., & Lee, F. H. (2018). Stability of tunnels in cement-admixed soft soils with spatial variability. Journal of Geotechnical and Geoenvironmental Engineering, (accepted)

Xiao, H., Lee, F. H., & Liu, Y. (2016). Bounding surface Cam-clay model with cohesion for cement-admixed clay. International Journal of Geomechanics, 17(1), 04016026.